ELSEVIER

Chemical Physics 259 (2000) 39–47

Chemical Physics

www.elsevier.nl/locate/chemphys

Production processes of H(D) atoms in the reactions of $NO(A^2\Sigma^+)$ with C_2H_2, C_2H_4, H_2O, and their isotopic variants

Hironobu Umemoto [a,*], Naoki Terada [a], Kunikazu Tanaka [a], Toshiyuki Takayanagi [b], Yuzuru Kurosaki [c], Keiichi Yokoyama [d]

[a] *Department of Chemical Materials Science, Japan Advanced Institute of Science and Technology, Asahidai, Tatsunokuchi, Nomi, Ishikawa 923-1292, Japan*

[b] *Advanced Science Research Center, Japan Atomic Energy Research Institute, Tokai, Ibaraki 319-1195, Japan*

[c] *Advanced Photon Research Center, Japan Atomic Energy Research Institute, Umemidai, Kizu, Soraku, Kyoto 619-0215, Japan*

[d] *Department of Materials Science, Japan Atomic Energy Research Institute, Tokai, Ibaraki 319-1195, Japan*

Received 9 May 2000

Abstract

The production of H(D) atoms was identified in the reactions of $NO(A^2\Sigma^+)$ with C_2H_2, C_2H_4, H_2O, and their isotopic variants. By measuring the Doppler profiles, the translational energies of H(D) atoms were determined. As for C_2H_2 and H_2O, around 1/4 of the $NO(A^2\Sigma^+)$ energy is partitioned into the translational mode, while the ratio is around 1/7 for C_2H_4. Such a large partitioning of the available energy into the translational mode cannot be explained by a C–H(O–H) bond rupture after an energy transfer. Nitrogen compounds, such as ONC_2H and HONO, must be produced as pair products. The measured translational energies are much larger than those statistically expected, suggesting that the intermediate species are short-lived. No large isotope effect was observed in the average translational energies or in the relative yields. Quantum effects, such as tunneling, do not play important roles. Ab initio molecular orbital calculations were carried out to characterize these reactive processes.

1. Introduction

Nitric oxide is sometimes called a "pet" molecule among the spectroscopists [1]. This may not be the case for researchers on chemical reaction dynamics. There have been numerous studies on the spectroscopy of NO molecules from vacuum ultraviolet to far infrared [2]. There have also been many studies on the determination of the rate constants for the overall quenching of the first excited $NO(A^2\Sigma^+)$ molecules [3–11]. However, few studies have contributed to the identification of the exit channels. Mauldin and Ravishankara observed the production of $O(^3P)$ in the reaction of $NO(A^2\Sigma^+)$ with O_2 [12]. The production of $N_2(A^3\Sigma_u^+)$ has been suggested in the quenching of $NO(A^2\Sigma^+, v' = 4)$ by N_2, very recently [13]. These should be the only systems in which the exit channels are identified, except for a few final product analysis studies [14,15]. Theoretical studies have not been carried out extensively, either.

Furlanetto et al. measured the cross-sections for the quenching of $NO(A^2\Sigma^+)$ by some saturated and unsaturated hydrocarbons over a wide temperature range [8]. The cross-sections by CH_4 and C_2H_6 are small even over 1000 K, while those by

* Corresponding author. Fax: +81-761-51-1655.
E-mail address: umemoto@jaist.ac.jp (H. Umemoto).

0301-0104/00/$ - see front matter
PII: S0301-0104(00)00184-1

C_2H_2 and C_2H_4 are large and show moderate decreases with the increase in temperature. In order to explain such a temperature dependence, they have proposed that the quenching proceeds via resonant or near-resonant electronic energy transfer. However, it is not clear what happens after the energy transfer. Since the electronic energy of $NO(A^2\Sigma^+)$ is larger than or comparable to the C–H bond strength, the quenchers may decompose after energy transfer. Internal conversion from the surface correlating to NO + triplet state hydrocarbons to the electronic ground state may also take place. In such a case, some closed-shell nitrogen compounds, such as ONC_2H, may be produced. It is desired to make clear the latter half of the reaction.

The lack of the experimental studies on the identification of the exit channels may partly be because the fluorescence range of $NO(A^2\Sigma^+)$ is very wide from ultraviolet to visible. It is difficult to employ a usual laser induced fluorescence technique to identify the product species. The resonance enhanced multiphoton ionization technique may be applied, but since NO can easily be ionized, the mass separation of the ions is critical. These problems can be overcome by monitoring the emission in the vacuum ultraviolet region. Atomic hydrogen can easily be detected by observing the Lyman-α fluorescence after two-photon excitation [16,17]. Then, the detection of atomic hydrogen produced in the reaction of $NO(A^2\Sigma^+)$ should be a break-through for the study of the reactions of excited NO molecules.

In the present study, the production of H(D) atoms was identified in the reactions of $NO(A^2\Sigma^+)$ with C_2H_2, C_2H_4, H_2O, and their isotopic variants. Quenching processes by these species have been reported to be very efficient [3,7–10].

2. Experimental

The experimental apparatus and the procedure were similar to those described elsewhere [18,19]. Ground state NO molecules were excited to the $A^2\Sigma^+$, $v' = 0$ state with a frequency double output of a YAG laser pumped dye laser (Quanta-ray, PDL-3/GCR-170). The excitation wavelength was fixed at 226.3 nm in most cases. This wavelength corresponds to the head of the Q_1 branch of the (0,0) band [3]. Some experiments were carried out at 226.1 nm to excite $R_1(8)$. The typical pulse energy was 0.7 mJ. Excited NO molecules react with hydride(deuteride) molecules, such as C_2H_2 and C_2D_2, to produce H(D) atoms. After a short time delay, typically 100 ns, H(D) atoms were detected with a frequency double output of another YAG laser pumped dye laser (Lambda Physik, LPD3000E and Quanta-ray, GCR-170). The typical pulse energy of the doubled output of the probe laser was 0.3 mJ. This laser pulse was focused into the interaction region by using a 200 mm focal-length lens. The pump and probe laser beams were aligned collinearly. Ground state H(D) atoms were excited to the 2^2S state with the two-photon scheme at 243.2 (243.0) nm. These excited H(D) atoms were then collisionally relaxed to the near-by 2^2P state that fluoresces vacuum ultraviolet light at 121.6 (121.5) nm. The vacuum ultraviolet fluorescence was detected with a solar-blind photomultiplier tube (Hamamatsu Photonics, R1459) through an MgF_2 window and an interference filter (Acton Research, 122-N). The photomultiplier signal was amplified by a preamplifier (Stanford Research Systems, SR240) and processed with a boxcar averager-gated integrator system (Stanford Research Systems, SR280/SR250). Doppler profiles of H(D) atoms were measured by scanning the wavelength of the probe laser. The bandwidth (0.5 cm^{-1}) of the doubled output of the probe laser was determined by measuring the Doppler profiles of H atoms under completely thermalized conditions. The typical total pressure was 40 Pa. There was no change in the Doppler profiles when this pressure was halved.

In the quenching rate constant measurements, just one laser was used. NO was excited via the (0,0) band of the A–X system, while the temporal profiles of the (0,3) band emission were monitored with a photomultiplier tube (Hamamatsu, R106UH) through a monochromator (JASCO, CT-25CP). The (0,3) band was chosen in order to avoid any problems caused by radiation trapping [8]. The slits of the monochromator were opened widely, 1 mm. Then, the collisional rotational re-

laxation does not appear as electronic quenching. A digital oscilloscope (LeCroy, 9450A) was used to average the decay profiles. All the measurements were carried out at 293 ± 2 K.

NO (Sumitomo Seika, 99.999%) and C_2H_4 (Sumitomo Seika, 99.9%) were used from cylinders without further purification. C_2D_4 was the product of ICON Stable Isotopes (isotopic purity 99%). Distilled and deionized H_2O was used after being degassed under vacuum. D_2O was the product of Aldrich (isotopic purity 99.9%). $C_2H_2(C_2D_2)$ was synthesized from CaC_2 (Katayama Kagaku) and $H_2O(D_2O)$.

3. Experimental results

The rate constants for the deactivation of $NO(A^2\Sigma^+)$ were determined under pseudo-first-order conditions. NO pressure was kept constant, 13 Pa, while the quencher pressure was changed between 0 and 90 Pa. Measurements with Ar buffer gas were also carried out but there was no difference in the decay rates. The emission intensity from $NO(A^2\Sigma^+)$ decreased exponentially against time. The decay rate increased linearly with the increase in the reactant gas pressure. From the slopes, it is possible to determine the absolute rate constants for the deactivation. The results are summarized in Table 1. The error limits are the standard deviations (1σ). The result for H_2O is in good agreement with the former literature values [3,7,9,10]. The results for C_2H_4 and C_2H_2 are also in fair agreement with those reported by Furlanetto et al. [8]. All the rate constants are large and gas kinetic, suggesting the absence of activation barriers. The lack of large isotope effects is also consistent with this model.

Figs. 1 and 2 show the Doppler profiles of H(D) atoms produced in the reaction of $NO(A^2\Sigma^+)$ with C_2H_2 and D_2O, respectively. Similar results were obtained for other species. The profiles for $C_2H_2(C_2D_2)$ and $C_2H_4(C_2D_4)$ can be approximated with gaussian functions, while that for $H_2O(D_2O)$ cannot. In other words, the velocity distribution for $H_2O(D_2O)$ cannot be represented by a Maxwell distribution at one temperature. Here, anisotropy in the velocity distribution cannot be important because $NO(A^2\Sigma^+)$ molecules may rotate many times during its lifetime. The Doppler profiles showed no dependence on the rotational energy of $NO(A^2\Sigma^+)$. H(D) atoms observed in the present system are not the direct photolysis products, because no H(D) atoms could be detected when the pump laser was detuned to the NO γ system. McGee and Heicklen have observed polymerization when C_2H_2 was exposed to the radiation from a low-pressure cadmium arc

Table 1
Rate constants for the deactivation of $NO(A^2\Sigma^+)$ at room temperature in units of 10^{-10} cm^3 s^{-1}

	This work	Literature values
C_2H_2	1.64 ± 0.05	1.89 ± 0.03[a]
C_2D_2	1.47 ± 0.03	
C_2H_4	3.04 ± 0.07	4.16 ± 0.26[a]
C_2D_4	2.95 ± 0.06	
H_2O	7.51 ± 0.15	7.58 ± 0.71[b], 8.00 ± 0.37[c], 8.08 ± 0.75[d], 8.97 ± 0.46[e]
D_2O	6.22 ± 0.23	

[a] Furlanetto et al. [8].
[b] McDermid and Laudenslager [3].
[c] Drake and Ratcliffe [7].
[d] Zhang and Crosley [9].
[e] Paul et al. [10].

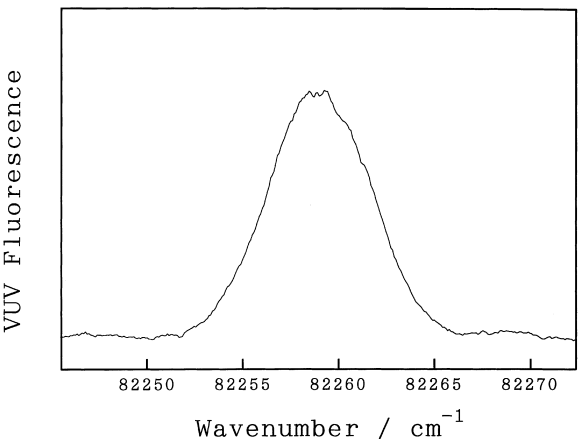

Fig. 1. Doppler profile of H atoms formed in the reaction of $NO(A^2\Sigma^+)$ with C_2H_2. The pressures were 30 Pa for NO and 10 Pa for C_2H_2. The photolysis-probe delay time was 100 ns.

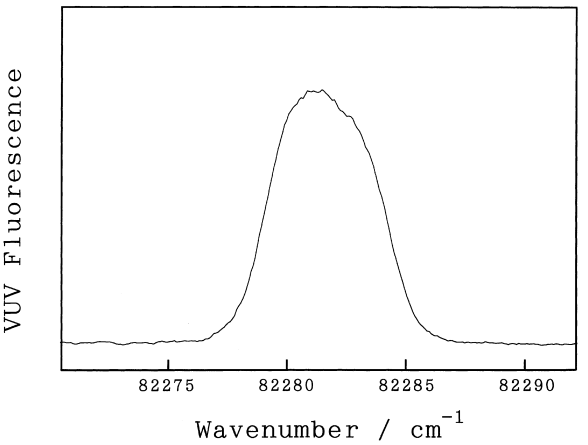

Fig. 2. Doppler profile of D atoms formed in the reaction of $NO(A^2\Sigma^+)$ with D_2O. The pressures were 10 Pa both for NO and D_2O. The photolysis-probe delay time was 100 ns.

Table 2
Average translational energies calculated from the second moments of the Doppler profiles and the statistically expected values in kJ mol^{-1}

Reactant	Measured	Statistical (prior)	Exothermicity
C_2H_2	133 ± 6	39	246
C_2D_2	130 ± 5		
C_2H_4	73 ± 4	34	297
C_2D_4	78 ± 3		
H_2O	113 ± 7	49	238
D_2O	108 ± 8		

[14]. This must be caused by the irradiation at 214.4 nm rather than at 226.5 nm. Table 2 summarizes the translational energies of H(D) atoms calculated from the second moments of the Doppler profiles. The computational procedure is the same as that employed by Matsumi et al. [20]. Since the profiles for $C_2H_2(C_2D_2)$ and $C_2H_4(C_2D_4)$ are near gaussian, there was no change when the translational energies were calculated from the half-widths.

The relative yields of H(D) atoms were also measured. The H/D signal ratios were measured for the 1:1 mixtures of C_2H_2/C_2D_2, C_2H_4/C_2D_2, C_2H_2/C_2D_4, and C_2H_4/C_2D_4. Since the overall rate constants are known, it is possible to convert these ratios into relative yields. The results were 1.4 ± 0.3 for C_2H_4 and 1.3 ± 0.3 for C_2D_4, when the yields for C_2H_2 and C_2D_2 are assumed to be unity. Similar results were obtained for H_2O and D_2O. The relative yields were 0.9 ± 0.2 and 0.8 ± 0.3, respectively.

4. Calculations

In order to understand the quenching mechanisms and reaction pathways of hydrogen atom production, we have carried out ab initio molecular orbital calculations. The adiabatic potential energy surfaces for $NO + C_2H_2$, C_2H_4, and H_2O were calculated. The computational procedure is as follows: The N–C or N–O internuclear distance was fixed to a certain value in the range of 0.13–0.30 nm. Other internal coordinates were optimized with respect to the total electronic energy of the ground state under Cs symmetry constraint. The electronic energies of the excited states were calculated by assuming the same geometries. The geometry optimization was carried out at the unrestricted Hartree–Fock (UHF) level with Dunning's correlation-consistent polarized valance double-zeta (cc-pVDZ) basis set [21] using the GAUSSIAN 94 program [22]. At each point of the N–C or N–O distance, the state-averaged complete-active-space self-consistent-field (SA-CASSCF) calculations were performed with the MOLCAS program [23]. The active space was carefully chosen so as that sufficiently smooth potential energy curves can be obtained but with less computational costs. In the case of $NO + C_2H_2$, for example, nine electrons were distributed among nine active orbitals $(5a' + 4a'')$ which include NOπ, NOπ^*, O2p, N2p, N3s, two CCπ, and two CCπ^*. The lowest 10 states were included in the averaging for both A′ and A″ symmetry of electronic states. Because the $NO(A^2\Sigma^+)$ state is Rydberg in character (3sσ), it is necessary to supplement the cc-pVDZ basis set with diffuse functions. In order to describe the $NO(A^2\Sigma^+)$ Rydberg state properly, 3s and 3p Rydberg basis functions were included with the following exponents [24]: N(3s) = 0.028, N(3p) = 0.025, O(3s) = 0.032, O(3p) = 0.020.

The potential energy curves thus calculated are plotted in Figs. 3–5. Since the CASSCF method

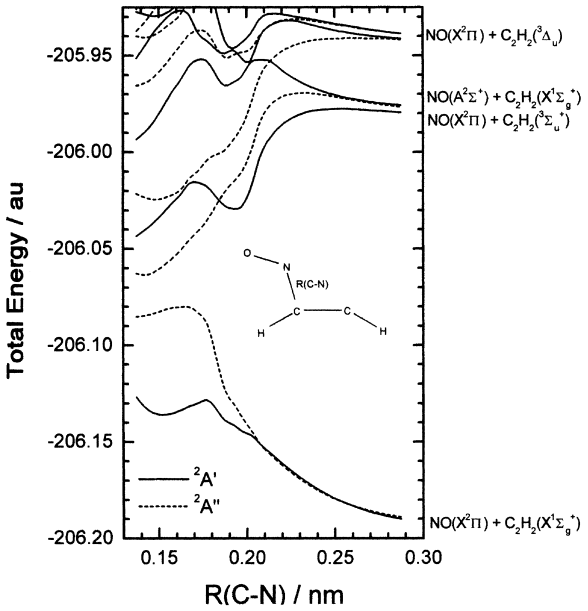

Fig. 3. Adiabatic potential energy curves in Cs symmetry for the $NO + C_2H_2$ system as a function of the N–C distance calculated by the SA-CASSCF method, in which nine electrons were distributed among nine active $(5a' + 4a'')$ orbitals.

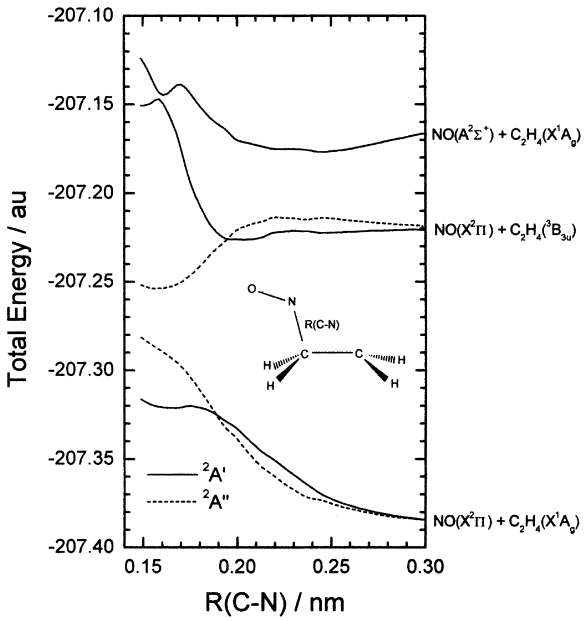

Fig. 4. Adiabatic potential energy curves for the $NO + C_2H_4$ system as a function of the N–C distance calculated by the SA-CASSCF method, in which nine electrons were distributed among 10 active $(7a' + 3a'')$ orbitals.

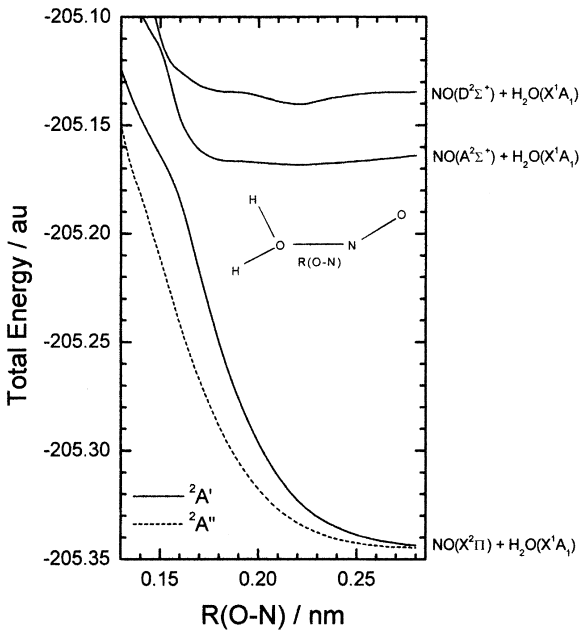

Fig. 5. Adiabatic potential energy curves for the $NO + H_2O$ system as a function of the N–O distance calculated by the SA-CASSCF method, in which nine electrons were distributed among 10 active $(6a' + 4a'')$ orbitals.

does not include a large amount of dynamical electron correlation, the calculated potential energy curves are probably in a qualitative level. However, it should be emphasized that the calculated vertical energy differences (0.21–0.22 a.u. for three systems) between the $NO(X^2\Pi)$ and $NO(A^2\Sigma^+)$ states reasonably agree with the more accurate value (0.206 a.u.), which was obtained from a large-scale multireference configuration interaction calculation with the large basis set [25].

The translational energies of H atoms expected in a simple statistical theory were calculated. The procedure is the same as that employed elsewhere [17,26]. The available energy was assumed to be partitioned into all the degrees of freedom in proportion to their statistical weights. No barriers were assumed, both in the entrance and in the exit. The exothermicity for the reactions of C_2H_2 and C_2H_4 was calculated at the MP2(full)/cc-pVDZ level of theory, while that for H_2O can be calculated from the experimentally obtained enthalpies of formation [27]. The results are as follows:

$$NO(A^2\Sigma^+) + C_2H_2 \rightarrow ONC_2H + H + 246\ kJ\,mol^{-1},$$

$$NO(A^2\Sigma^+) + C_2H_4 \rightarrow ONC_2H_3 + H + 297\ kJ\,mol^{-1},$$

$$NO(A^2\Sigma^+) + H_2O \rightarrow HONO + H + 238\ kJ\,mol^{-1}.$$

The three body dissociation processes, such as $NO(A^2\Sigma^+) + H_2O \rightarrow NO + OH + H$, are much less exothermic (or even endothermic) and cannot explain the large translational energies of H atoms observed. The harmonic vibrational frequencies of the products were calculated at the MP2(full)/cc-pVDZ level of theory. The results are as follows:

ONC_2H : 212, 307, 621, 664, 691, 911, 1431, 2107, and 3502 cm^{-1},

ONC_2H_3 : 173, 340, 613, 689, 906, 975, 1012, 1159, 1278, 1415, 1498, 1683, 3206, 3224, and 3330 cm^{-1}.

The experimental values were employed for HONO: 3590, 1698, 1264, 793, 598, and 544 cm^{-1} [28]. The calculated results for the average translational energies are given in Table 2.

In the present systems, there may be exit barriers, because the reverse reactions are those between an atom and a closed-shell molecule. For example, in the reaction of H with HONO to produce H_2O and NO, the activation barrier is calculated to be as high as 16 $kJ\,mol^{-1}$ [29]. However, even taking into account the presence of such high barriers, the translational energies of atomic hydrogen are too large compared to the statistically expected ones. The highly nonstatistical behavior suggests that the intermediate species are short-lived.

5. Discussion

McGee and Heicklen have applied a final product analysis technique to investigate the reactions of $NO(A^2\Sigma^+)$ with C_2H_2 and C_2H_4 [14]. They concluded that the quenching by C_2H_4 proceeds via a molecular elimination process because they could not detect HCN or HCHO as products. This is in contradiction to the present results of the H atom production. However, it should be remembered that the main products in the C_2H_2 and C_2H_4 systems were solid deposits which were not quantified. In addition, their results on the quenching efficiencies by H_2, CH_4, and C_2H_6 have not been reproduced in more recent studies [4,7,8,15].

The production of the triplet states of C_2H_2 and C_2H_4 is energetically possible. The lowest triplet levels of these molecules are much lower than the energy level of $NO(A^2\Sigma^+)$ [30,31]. Furlanetto et al. have proposed that these processes should be the main exit channels [8]. Similar production of triplet state molecules has been confirmed in the quenching of $Hg(6^3P_1)$ and $Cd(5^3P_J)$ by unsaturated hydrocarbons [32,33]. However, atomic hydrogen is surely produced in the present systems. This cannot be attributed to the decomposition of triplet state hydrocarbons after energy transfer because the observed translational energies are too large. In order to make this point clear, we have carried out molecular orbital calculations.

Fig. 3 shows the adiabatic potential energy curves in Cs symmetry for the $NO + C_2H_2$ system as a function of the N–C distance calculated by the SA-CASSCF method. The energy levels for the $NO(A^2\Sigma^+) + C_2H_2(X^1\Sigma_g^+)$ and $NO(X^2\Pi) + C_2H_2(^3\Sigma_u^+)$ asymptotes are very close. The energy difference between them corresponds to that for a vertical transition. An efficient nonadiabatic transition from the $NO(A^2\Sigma^+) + C_2H_2(X^1\Sigma_g^+)$ potential to the $NO(X^2\Pi) + C_2H_2(^3\Sigma_u^+)$ potential is expected at a long-range region. Here, it should be noted that the potential curve correlating to $NO(A^2\Sigma^+) + C_2H_2(X^1\Sigma_g^+)$ is repulsive, while that correlating to $NO(X^2\Pi) + C_2H_2(^3\Sigma_u^+)$ is attractive. The intermediate radical produced by the

nonadiabatic transition may live during a few vibrational periods. During the lifetime, it may relax to the ground state via an internal conversion. Of course, dissociation to triplet state C_2H_2 and ground state NO may compete. A local minimum is seen on the lowest $^2A'$ potential curve at $R(C–N) \approx 0.15$ nm. This local minimum corresponds to the intermediate radical (ON(H)C=CH) in which the N atom of NO adds to one of the C atoms of C_2H_2. This intermediate radical is unstable. It may undertake the steps of isomerization, but the more probable exit channel is the dissociation into either $NO(X^2\Pi) + C_2H_2(X^1\Sigma_g^+)$ or H + ONC≡CH. In order to explain the large translational energy of H atoms, none of the intermediate species leading to the production of H atoms are long-lived to permit energy randomization.

The quenching mechanism for C_2H_4 is probably similar to that for C_2H_2. The potential energy curves for the $NO + C_2H_4$ system is shown in Fig. 4. At the entrance channel, the potential curve for this system is more attractive than that for C_2H_2. This accounts for the larger rate constant for the quenching by C_2H_4 compared to that by C_2H_2. There are two potential energy curves which correlate asymptotically to $NO(X^2\Pi) + C_2H_4(^3B_{3u})$ below the $NO(A^2\Sigma^+) + C_2H_4(^1A_g)$ state. There are potential wells in both surfaces. In addition, a shallow local minimum is seen on the lowest $^2A'$ potential energy curve, corresponding to an intermediate radical on the ground state. These features are similar to those for the $NO + C_2H_2$ system. The formation of H atoms can take place through the nonadiabatic transition from the initial surface to the surfaces correlating to $NO(X^2\Pi) + C_2H_4(^3B_{3u})$ followed by a C–H bond rupture on the ground state surface.

The feature of the potential energy curves for the $NO + H_2O$ system is very different from those for $NO + C_2H_2$ and $NO + C_2H_4$ and is rather simple as is shown in Fig. 5. This is simply because the energy difference between the excited and ground states of H_2O is much larger than that between $NO(A^2\Sigma^+)$ and $NO(X^2\Pi)$. The lowest excited state of H_2O is the 3s-Rydberg state. The interaction between the ground state $NO(X^2\Pi)$ and $H_2O(X^1A_1)$ is found to be strongly repulsive. This means that no long-lived intermediate complex is formed in the $NO + H_2O$ system. Also, it is seen a strong avoided crossing between the lowest two $^2A'$ potential energy curves at $R(O–N) \approx 0.16$ nm. The most probable quenching mechanism of $NO(A^2\Sigma^+) + H_2O(X^1A_1)$ is the nonadiabatic transition from the second lowest $^2A'$ surface to the lowest $^2A'$ surface. Judging from the extremely large quenching cross-section, this transition must be very efficient. On the lowest $^2A'$ surface, H atoms shall be produced directly, because the $H(^2S) + HONO(^1A')$ asymptotes correlate adiabatically to the $^2A'$ state of $NO(X^2\Pi) + H_2O(^1A_1)$ within Cs symmetry constraint; i.e., planar geometry constraint. In order to confirm this, we have calculated the lowest $^2A'$ potential energy surface as functions of the OH and ON internuclear distances at the UHF/cc-pVDZ level of theory. Other internal coordinates were fixed to the values for which the avoided crossing occurs ($R(O–N) \approx$ 0.16 nm). The contour map of this surface is plotted in Fig. 6. As expected, it is found that the lowest $^2A'$ potential energy surface adiabatically correlates to both the $NO(X^2\Pi) + H_2O(X^1A_1)$ and $H(^2S) + HONO(^1A')$ products. The shaded area shown in Fig. 6 corresponds to the region where nonadiabatic transitions from the second lowest $^2A'$ state to the lowest $^2A'$ state are expected to occur. From Fig. 6, we can understand that the dissociation into $H(^2S) + HONO(^1A')$ is possible.

For further discussion, information on the absolute yields for the production of H atoms is desired. The saturation-depletion technique is useful to determine the ratios of physical and chemical processes for atomic species [34,35]. However, for molecular species, vibrationally excited ground state molecules may be produced in physical processes. Vibrational moderators which do not quench $NO(A^2\Sigma^+)$ are required. CH_4, and possibly CF_4, should be useful for such purpose. Experiments on the *cis–trans* isomerization of CHD=CHD should also be informative.

Recently, Bakker et al. have proposed that stepwise photodissociation of NO can be a good source of metastable atomic nitrogen, $N(^2D)$ [36]. In their technique, NO is excited to the $A^2\Sigma^+$ state at the first step. In the second step, $NO(A^2\Sigma^+)$ is photodissociated at 339 nm to produce $N(^2D)$.

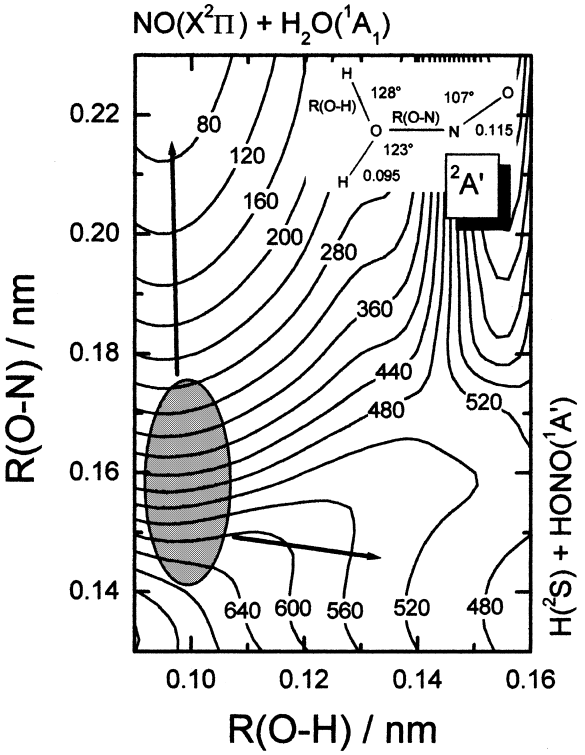

Fig. 6. Contour map of the two-dimensional potential energy surface of the lowest $^2A'$ state for the $NO + H_2O$ system as functions of the O–H and O–N internuclear distances calculated at the UHF/cc-pVDZ level of theory. Other internal coordinates are fixed as shown in the inserted figure. It is expected that nonadiabatic transitions from the upper $^2A'$ state to the lower $^2A'$ state occur in the shaded region. The zero of the energy is set to the $NO(X^2\Pi) + H_2O$ asymptotes. The contour increment is 40 kJ mol^{-1}.

This technique is unique and useful because velocity aligned beams of $N(^2D)$ can be obtained. However, when this technique is applied to the identification of the reaction products of $N(^2D)$, care must be paid to the reactions of $NO(A^2\Sigma^+)$.

6. Conclusion

Quenching processes of $NO(A^2\Sigma^+)$ by C_2H_2, C_2H_4, H_2O, and their isotopic variants are all gas kinetic and H(D) atoms were identified as products. Three body dissociation processes, such as the production of $NO + OH + H$, are minor and only two body dissociation processes, such as $H + HONO$, take place. The translational energies of H(D) atoms are much larger than those statistically expected. In addition, in the case of $H_2O(D_2O)$, the velocity distribution cannot be represented by a Maxwell one. The intermediate states must be short-lived in all the cases. In the C_2H_2 and C_2H_4 systems, nonadiabatic transitions to the levels correlating to ground state NO and triplet state hydrocarbons may play important roles, while direct transition to the lowest $^2A'$ state should be dominant in the quenching by H_2O. No large H/D isotope effect could be observed suggesting that quantum effects are minor.

Acknowledgements

This work was partially defrayed by the Grant-in-Aid for Science Research (no. 11640501) from the Ministry of Education, Science, Sports, and Culture of Japan.

References

[1] A. Fujii, T. Ebata, M. Ito, J. Chem. Phys. 90 (1989) 6993.
[2] K.P. Huber, G. Herzberg, Molecular Spectra and Molecular Structure IV, Constants of Diatomic Molecules, Van Nostrand Reinhold, New York, 1979.
[3] I.S. McDermid, J.B. Laudenslager, J. Quant. Spectrosc. Radiat. Trans. 27 (1982) 483.
[4] Y. Haas, G.D. Greenblatt, J. Phys. Chem. 90 (1986) 513.
[5] G.A. Raiche, D.R. Crosley, J. Chem. Phys. 92 (1990) 5211.
[6] J.W. Thoman Jr., J.A. Gray, J.L. Durant Jr., P.H. Paul, J. Chem. Phys. 97 (1992) 8156.
[7] M.C. Drake, J.W. Ratcliffe, J. Chem. Phys. 98 (1993) 3850.
[8] M.R. Furlanetto, J.W. Thoman Jr., J.A. Gray, P.H. Paul, J.L. Durant Jr., J. Chem. Phys. 101 (1994) 10452.
[9] R. Zhang, D.R. Crosley, J. Chem. Phys. 102 (1995) 7418.
[10] P.H. Paul, J.A. Gray, J.L. Durant Jr., J.W. Thoman Jr., Chem. Phys. Lett. 259 (1996) 508.
[11] T. Hikida, T. Suzuki, Y. Mori, Chem. Phys. 118 (1987) 437.
[12] R.L. Mauldin III, A.R. Ravishankara, J. Phys. Chem. 90 (1986) 4923.
[13] J. Luque, D.R. Crosley, J. Phys. Chem. A 104 (2000) 2567.
[14] J.J. McGee, J. Heicklen, J. Chem. Phys. 41 (1964) 2977.
[15] J. Heicklen, J. Phys. Chem. 70 (1966) 2456.
[16] T.W. Hänsch, S.A. Lee, R. Wallenstein, C. Wieman, Phys. Rev. Lett. 34 (1975) 307.

[17] H. Umemoto, T. Nakae, H. Hashimoto, K. Kongo, M. Kawasaki, J. Chem. Phys. 109 (1998) 5844.
[18] H. Umemoto, T. Asai, Y. Kimura, J. Chem. Phys. 106 (1997) 4985.
[19] H. Umemoto, N. Hachiya, E. Matsunaga, A. Suda, M. Kawasaki, Chem. Phys. Lett. 296 (1998) 203.
[20] Y. Matsumi, K. Tonokura, M. Kawasaki, H.L. Kim, J. Phys. Chem. 96 (1992) 10622.
[21] T.H. Dunning Jr., J. Chem. Phys. 90 (1989) 1007.
[22] M.J. Frisch, G.W. Trucks, H.B. Schlegel, P.M.W. Gill, B.G. Johnson, M.A. Robb, J.R. Cheeseman, T. Keith, G.A. Petersson, J.A. Montgomery, K. Raghavachari, M.A. Al-Laham, V.G. Zakrzewski, J.V. Ortiz, J.B. Foresman, J. Cioslowski, B.B. Stefanov, A. Nanayakkara, M.C. Challacombe, Y. Peng, P.Y. Ayala, W. Chen, M.W. Wong, J.L. Andres, E.S. Replogle, R. Gomperts, R.L. Martin, D.J. Fox, J.S. Binkley, D.J. Defrees, J. Baker, J.P. Stewart, M. Head-Gordon, C. Gonzalez, J.A. Pople, GAUSSIAN 94 (1995) Gaussian, Pittsburgh, PA.
[23] MOLCAS, ver. 4, K. Andersson, M.R.A. Blomberg, M.P. Fulscher, G. Karlstrom, R. Lindh, P.-A. Malmqvist, P. Neogrady, J. Olsen, B.O. Roos, A.J. Sadlej, M. Schutz, L. Seijo, L. Serrano-Andres, P.E.M. Siegbahn, P.-O. Widmark, Lund University, Sweden, 1997.
[24] R. de Vivie, S.D. Peyerimhoff, J. Chem. Phys. 89 (1988) 3028.
[25] J.A. Sheehy, C.W. Bauschlicher Jr., S.R. Langhoff, H. Partridge, Chem. Phys. Lett. 225 (1994) 221.
[26] H. Umemoto, T. Asai, H. Hashimoto, T. Nakae, J. Phys. Chem. A 103 (1999) 700.
[27] D.R. Lide (Ed.), CRC Handbook of Chemistry and Physics, 76th ed., CRC Press, Boca Raton, FL, 1995–1996.
[28] G. Herzberg, Molecular Spectra Molecular Structure III, Electronic Spectra and Electronic Structure of Polyatomic Molecules, Van Nostrand Reinhold, Princeton, NJ, 1967.
[29] C.-C. Hsu, M.C. Lin, A.M. Mebel, C.F. Melius, J. Phys. Chem. A 101 (1997) 60.
[30] Y. Yamaguchi, G. Vacek, H.F. Schaefer III, Theor. Chim. Acta 86 (1993) 97.
[31] B. Gemein, S.D. Peyerimhoff, J. Phys. Chem. 100 (1996) 19257.
[32] W.H. Breckenridge, H. Umemoto, Adv. Chem. Phys. 50 (1982) 325.
[33] S. Tsunashima, S. Sato, Rev. Chem. Intermed. 2 (1979) 201.
[34] H. Umemoto, N. Ohsako, Bull. Chem. Soc. Jpn. 69 (1996) 2185.
[35] S.A. Mitchell, P.A. Hackett, D.M. Rayner, M. Flood, J. Chem. Phys. 86 (1987) 6852.
[36] B.L.G. Bakker, A.T.J.B. Eppink, D.H. Parker, M.L. Costen, G. Hancock, G.A.D. Ritchie, Chem. Phys. Lett. 283 (1998) 319.